

Influence of microstructure on hydrogen diffusion and impedance of IF-steel

A. Begić Hadžipašić^{1*}, J. Malina¹, Š. Nižnik²

¹University of Zagreb, Faculty of Metallurgy, Aleja narodnih heroja 3, 44103 Sisak, Croatia

²Technical University of Košice, Faculty of Metallurgy, Letná 11, 04200 Košice, Slovak Republic

Received 2 September 2011, received in revised form 27 December 2011, accepted 2 February 2012

Abstract

In this work the influence of microstructure on hydrogen diffusion and impedance of interstitial free (IF) steel was studied. The permeation experiments have shown that electrochemical corrosion of IF-steel in 2M H₂SO₄ results in evolution and absorption of hydrogen atoms in the material. The obtained diffusion parameters indicate the connection of transport of diffusible hydrogen with traps presented in examined interstitial free steel.

The analysis of experimental EIS data of examined sample carried out by model of the most common equivalent electric circuit R (QR) has shown that simulated curves match with experimental curves and that compact layer obtained on IF-steel cannot present a barrier for hydrogen diffusion because of its small thickness.

By metallographic and SEM examinations the inclusions of square shape were registered and EDS analysis revealed the presence of titanium nitrides, which act as irreversible hydrogen traps towards suppression of fish-scales phenomenon in enamelling process.

Key words: interstitial free (IF) steel, hydrogen diffusion, hydrogen traps, microstructure, impedance

1. Introduction

Interstitial free (IF) steels are steels with extraordinary shape ability which is why they have found their application in the automotive industry. In recent decades the progress in the production of IF-steel has been accomplished by achieving a very low concentration of interstitial elements (total C \leq 30 ppm and total N \leq 40 ppm) [1]. These interstitial elements combine with the stabilizing elements such as Ti or Nb, creating the different types of carbides, nitrides, sulphides, carbonitrides and carbosulphides [2]. This phenomenon of precipitation in ferritic steels enables them to be interstitial free and resistant to ageing [3–5].

Although IF-steels meet the stringent requirements of the automotive industry, a major drawback is their low tensile strength, which is partially resolved by applying various metallurgical phenomena [6]. Namely, various substitution elements like P, Mn and Si were added in order to increase the tensile strength, which

resulted in gaining high-strength interstitial free (IF-HS) steels. Also, a method of grain refinement with Nb has been applied in order to increase strength.

However, in spite of all this, the maximum value of tensile strength that can be achieved in IF-steel is 450 MPa, which is very low compared to modern high-strength structural auto-steels such as dual phase steels (DP), transformation induced plasticity steels (TRIP) and twinning induced plasticity steels (TWIP) [1, 7–9].

In this work the influence of microstructure on hydrogen diffusion and impedance of IF-steel was studied in order to gain insight in characterization of low-alloyed steel products before the enamelling process. Namely, it is known from literature that defects called fish scales can occur on enamel coatings, if the hydrogen that penetrates through the metal during the enamelling is not captured in irreversible traps.

Since it is necessary to determine the hydrogen diffusion coefficient and the type and amount of traps to define the influence of microstructure on hydrogen dif-

*Corresponding author: tel.: + 385 44 533 379 (local 224); fax: + 385 44 533 378; e-mail address: begic@simet.hr

Table 1. Chemical composition of examined IF-steel (wt.%)

| C | Mn | Si | P | S | Al | N | Nb | Ti | Mo | V |
|-------|-------|-------|-------|-------|-------|-------|-------|-------|-------|-------|
| 0.002 | 0.270 | 0.008 | 0.012 | 0.015 | 0.043 | 0.009 | 0.050 | 0.048 | 0.003 | 0.002 |

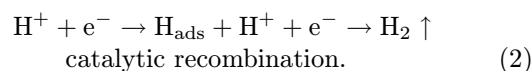
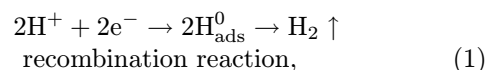
fusion, in this work electrochemical method of measuring hydrogen diffusion and permeation through a steel membrane according to Devanathan and Stachurski is applied [10].

2. Experimental

The samples used in this study were made of IF-steel which belongs to a group of cold rolled sheets marked as DC06EK according to EN 10209/96 (Table 1). Such sheets are produced by cold rolling from special killed steel, and are applied in the automotive industry for deep drawing for conventional enamelling. However, unlike conventional cold-rolled sheets for enamelling, IF-steel has a better enamelling ability, because the technology of its production is based on reducing the possibility of creating places that serve as reversible hydrogen traps.

In order to investigate the tendency toward hydrogen embrittlement, it is necessary to hydrogenate the sample using one of the electrochemical techniques. The penetration of hydrogen atoms through steel materials can be accelerated by the simple laboratory procedure of electrochemical examination of hydrogen diffusion in ferrous materials [10, 11]. For permeation experiments the sample was cut from IF-steel sheet of original thickness into plate with dimensions: (5 × 8 × 0.14) cm. The anodic (exit) side of the samples was coated with nickel, because the experimental conditions (medium and electrode potential) were controlled so that the surface at the oxidation side of metallic membrane remained passive or corrosion resistant. Before each measurement, the entry side of the sample was grounded with emery paper to a 600 grit finish, rinsed in distilled water, and degreased in ethanol. The experimental device for monitoring hydrogen diffusion through the metallic membrane consisted of a cell for hydrogen charging (entry part) and an oxidation cell (exit part), separated with a thin steel plate (sample-working electrode) [12]. The entry side of the sample was hydrogenated, so it was placed in contact with the cell filled with 2 mol l⁻¹ H₂SO₄ deaerated with nitrogen, while the anodic side was placed next to the anodic (exit) part filled with 1 mol l⁻¹ NaOH. In the anodic part saturated calomel electrode (SCE) was placed as reference electrode and Pt-electrode as counter electrode. The potential of steel membrane was maintained by Parstat Potentiostat/Galvanostat (Princeton Applied Research, USA) Model 2273 in the passivity area: + 200 mV vs. SCE.

In the entry part of the experimental device the hydrogen evolution occurs, which in one part recombines into the hydrogen molecule and releases in the form of gaseous hydrogen, while the second part of hydrogen diffuses through the steel membrane to the anodic part and oxidizes in H⁺-ions by the influence of applied potential (Eqs. (1) and (2)). The current flow between the steel membrane (working electrode) and counter electrode (Pt-electrode) is registered at potentiostat as permeation current I (μA), which presents the measure for the amount of hydrogen that diffuse through the steel membrane [13].



For the purpose of the research phase boundary electrode/electrolyte electrochemical impedance spectroscopy was applied [14, 15]. In order to perform impedance measurements sample of IF-steel in form of plate dimensions (3 × 2 × 0.14) cm was cleaned with abrasive grit No. 100, 220, 320, 400, 500 and 600, rinsed in distilled water and degreased in ethanol. Then the sample (working electrode) was immersed in the medium of 2 mol l⁻¹ H₂SO₄ in three-electrode glass cell in which saturated calomel electrode-SCE (reference electrode) and Pt-mesh (auxiliary electrode) were found. First, one-hour stabilization of open-circuit potential was started using potentiostat at room temperature $T = (19 \pm 2)^\circ\text{C}$. After that, two impedance measurements in the frequency range from 100 kHz to 10 mHz with amplitude of sinusoidal voltage of 5 mV were performed. The results were analysed using software ZSIMPWin3.21, and in processing the results arithmetic mean of impedance parameters is shown.

For the purpose of metallographic investigations of microstructural characteristics of non-hydrogenated IF-steel, the sample was cut in rolling direction and pressed by “SimpliMet®” machine for hot pressing of samples. The sample was then grounded (emery paper No. 400, 500, 600 and 800 grit) and polished by the “Buehler” automatic device for grounding and polishing. The sample prepared in such a way was observed by optical microscope with “Olympus GX 51” digital camera with system for automated picture analysis (AnalySIS® Materials Research Lab) to detect the inclusions. After that, the sample was etched by nital

Table 2. Hydrogen diffusion parameters of examined IF-steel

| Permeation | i_{ss} ($\mu\text{A cm}^{-2}$) | t_{lag} (s) | $n(\text{H}_2) \times 10^6$ (mol cm^{-2}) | $V(\text{H}_2) \times 10^3$ ($\text{cm}^3 \text{H}_2 \text{cm}^{-2}$) | $D \times 10^7$ ($\text{cm}^2 \text{s}^{-1}$) | $J_{ss} \times 10^{11}$ ($\text{mol cm}^{-2} \text{s}^{-1}$) | $C_{0R} \times 10^6$ (mol H cm^{-3}) |
|------------|---------------------------------------|------------------|---|--|--|---|--|
| 1st | 32.42 | 6096 | 1.54 | 34.54 | 5.36 | 33.60 | 87.76 |
| 2nd | 29.84 | 4980 | 1.74 | 38.98 | 6.55 | 30.92 | 66.09 |
| 3rd | 31.55 | 3708 | 1.22 | 27.33 | 8.81 | 32.70 | 51.96 |
| 4th | 30.64 | 3096 | 1.39 | 31.16 | 10.60 | 31.75 | 41.93 |

(5 % HNO_3 in ethanol) to record its microstructure.

SEM/EDS analysis of registered inclusions and microstructure of IF-steel was carried out by scanning electron microscope “Tescan Vega LSH” (Czech Republic) equipped with “Bruker” EDS spectrometer. The substructure of observed IF-steel was recorded by transmission electronic microscope TEM JEM 2000-FX equipped with LINK EDX and EELS analytic analyzer.

3. Results and discussion

On the basis of electrochemical diffusion measurements and taking into consideration the registered hydrogen current at the exit side of membrane I (μA) and working area A (cm^2), the permeation current density of atomic hydrogen $i(t)$ was calculated according to the following equation [13]:

$$i = \frac{I}{A} \quad (\mu\text{A cm}^{-2}) \quad (3)$$

and displayed as the function of diffusion time $i = f(t)$ (Fig. 1).

By the analysis of obtained results from diagram $i = f(t)$, atomic hydrogen permeation current density in steady-state i_{ss} , defined as asymptotic value at permeation curve, is determined. The i_{ss} value is established at the moment when all H-atoms that penetrate into the membrane ease out at the opposite side, where steady-state atomic hydrogen permeation flux is accomplished. Also, the following diffusion parameters have been calculated: diffusion coefficient D_{eff} , time t_{lag} , amount of hydrogen atoms in a steady-state that passed through a metal membrane n (H_2), the volume of hydrogen atoms at steady-state that passed through a metal membrane V (H_2), atomic hydrogen permeation flux at steady-state J_{ss} and the summation of the sub-surface concentration of hydrogen in interstitial lattice sites and reversible trap sites on the charging side of the sample C_{0R} [13]. These diffusion parameters were calculated for the four measurements (permeations) and are shown in Table 2.

In Fig. 1 the four permeation curves are shown: the first curve presents hydrogen transport through the metal membrane which has never been in contact

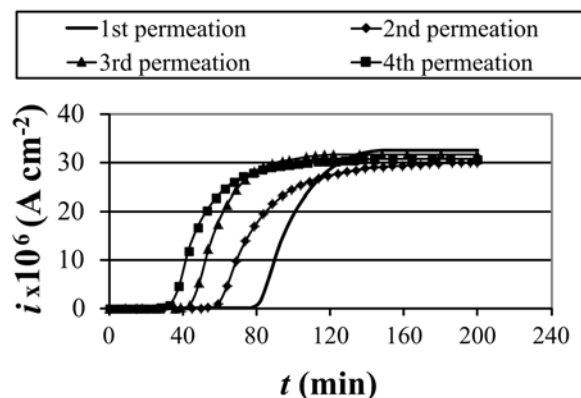


Fig. 1. Permeation current density of atomic hydrogen against diffusion time through membrane of IF-steel.

with corrosive medium, while the other permeation transients differ from the first because the membrane has already been in contact with medium and to some extent already hydrogenated.

It can be seen from Fig. 1 that hydrogen absorbed in IF-steel at first permeation transient needs 77 min to diffuse to the opposite side of the membrane. When all traps are filled (irreversible and reversible), steady-state flux of atomic hydrogen is established at the exit side of membrane, which can be seen as J_{ss} after 153 min. Every following permeation transient needs less time to reach the opposite side of the membrane, because only the reversible traps are slowing down the hydrogen transport [13]. This is evidenced by the obtained values of time delay t_{lag} listed in Table 2.

From the values in Table 2 it can be noticed that diffusion parameters are lower by three orders of magnitude than that in crystal lattice of α -Fe ($D_{Fe} = 1.28 \times 10^{-4} \text{cm}^2 \text{s}^{-1}$) [16], which means that lots of traps are present that slow down the transport of H-atoms through a membrane. Namely, it is known that increasing of D_{eff} and decreasing of C_{0R} strongly depend on hydrogen trapping, and traps are most frequently various defects in the material such as dislocations, grain boundaries, etc. [5, 11, 17].

Differences in calculated diffusion parameters between the first and the other transients are not very large, which leads to the conclusion that IF-steel has not got a large number of irreversible traps. That con-

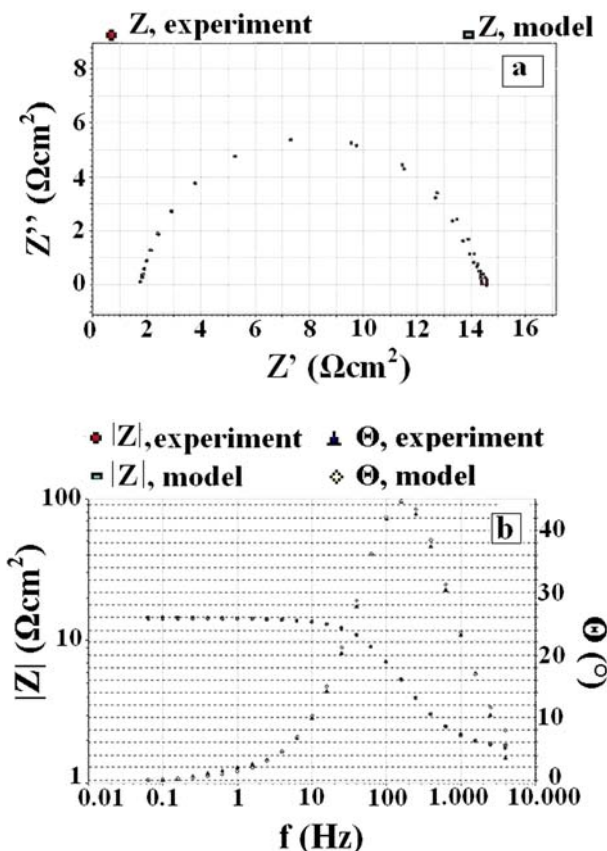


Fig. 2. a) Nyquist plot of IF-steel in medium of $2 \text{ mol l}^{-1} \text{ H}_2\text{SO}_4$, b) Bode plot of IF-steel in medium of $2 \text{ mol l}^{-1} \text{ H}_2\text{SO}_4$.

firm the permeation curves of examined steel, which have shown a steep slope. Namely, the permeation curves are sloping smoothly, indicating that the absorption of hydrogen in traps within the material is slower, and that in addition to reversible traps in the steel, there are also irreversible traps that permanently absorb hydrogen.

Nyquist and Bode impedance plot of tested IF-steel is shown in Fig. 2. Nyquist's plot gives the dependence of the imaginary part of impedance Z'' on the real part of impedance Z' , while Bode's plot gives the dependence of logarithm of the absolute value of impedance $|Z|$ and phase angle Θ on the logarithm of frequency f . For the sample of IF-steel two impedance measurements were carried out, whereby for processing impedance results, the arithmetic mean of obtained impedance parameters was used (Table 3).

The analysis of experimental EIS data of tested IF-steel conducted using the simplest model of the equivalent electrical circuit R (QR) showed that the simulated curves matched well with the experimental curves, as can be seen in Fig. 2 (the deviation is the order of 10^{-4}). In this model the resistance of charge transfer R_{ct} and the capacity of double layer C_{dl} are

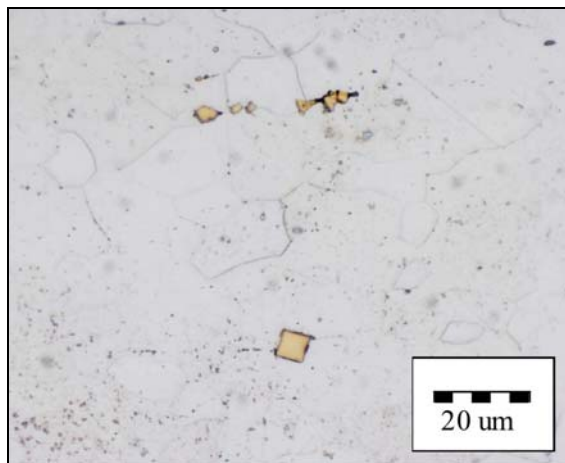


Fig. 3. Optical micrograph of microstructure of IF-steel etched by nital.

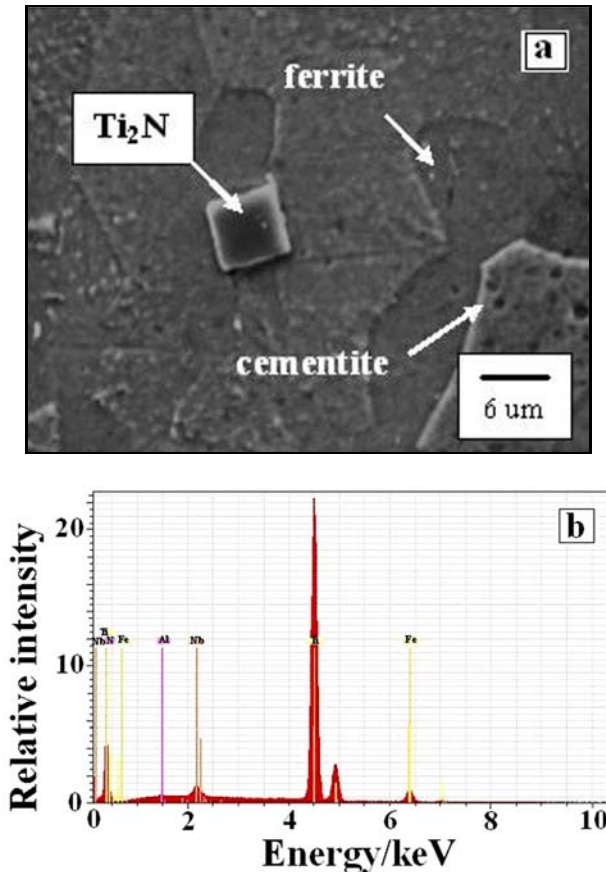
Table 3. Impedance parameters of IF-steel obtained by EIS-measurements

| E_{corr} vs. SCE (mV) | R_{el} ($\Omega \text{ cm}^2$) | $Q_{dl} \times 10^5$ ($\Omega^{-1} \text{ s}^n \text{ cm}^{-2}$) | n | R_{ct} ($\Omega \text{ cm}^2$) |
|-----------------------------------|---------------------------------------|---|------|---------------------------------------|
| -490 | 1.79 | 39.83 | 0.90 | 12.69 |

connected in parallel, and thus represent a passive electrode system. By measuring the impedance of the real system, deviation of capacity from the "pure capacity" can occur. Therefore, to adjust and replace the capacitor C , constant phase element of the double layer Q_{dl} is introduced, which is a combination of properties associated with the surface condition and electroactive substances. Therefore, R_{el} represents the uncompensated solution resistance (electrolyte resistance), and n the measure of the surface heterogeneity of the electrode [15, 18].

It is evident from Table 3 that IF-steel showed little resistance to charge transfer R_{ct} , which can be connected with a relatively easy development of hydrogen on the electrode surface and with the formation of the oxide layer of lesser thickness [19, 20]. Furthermore, the relatively high value Q_{dl} registered at IF-steel can be explained as a consequence of less compact passive layer which grows on the surface of the sample and therefore increases the capacity of the interface metal/oxide layer or within the passive layer. In other words, the resulting passive layer due to its small thickness cannot constitute a barrier to hydrogen diffusion through the membrane of IF steel.

IF-steel is ultra low carbon (0.002 % C) mild steel microalloyed with niobium and titanium (Table 1). As for the inclusions, IF-steel is a very clean material, al-



| Element | N | Ti | Fe | Nb | Al |
|---------|-------|-------|------|------|------|
| wt. % | 31.96 | 61.08 | 4.80 | 2.06 | 0.11 |
| at. % | 62.18 | 34.77 | 2.34 | 0.60 | 0.11 |

Fig. 4a,b. EDS analysis of square inclusion in IF-steel.

most with no globular inclusions, while the elongated inclusions are not registered. It is associated with the fact that investigated IF-steel has a low content of manganese and sulphur, so elongated MnS inclusions are not expected. However, its etching in nital showed inclusions of square shape (Fig. 3), whose EDS analysis has proven to be a titanium nitride Ti_2N (Fig. 4). The appearance of titanium nitride was to be expected, since the IF-steel in its chemical composition has the highest amount of titanium and niobium (Table 1), which are known as strong producers of carbide and nitride [2].

The microstructure of IF steel consists of large ferrite grains surrounded by a small number of cementite particles (Figs. 3 and 4). Due to the size of ferrite grains in the microstructure of this material, grain boundaries that are ideal reversible traps for hydrogen are more pronounced. However, here irreversible hydrogen traps that appear in the form of carbide, carbonitride and already mentioned titanium nitride are more significant. Namely, IF-steels are produced by cold rolling of special killed steel, and are applied

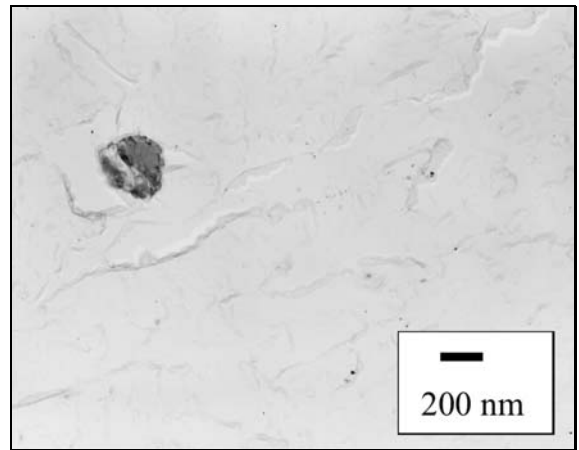


Fig. 5. TEM micrograph of particles in C-replica.

for deep drawing in the conventional enamelling process. After the process of applying enamel, it anneals at a temperature of 800–850 °C and then it is cooled. At the same time, the solubility of hydrogen in steel gradually decreases, hydrogen progressively migrates to the phase boundary steel/enamel, causing undesirable phenomena called fish-scales [5, 21]. Therefore, IF-steel in its microstructure must bind carbon in cementite, and with a sufficient amount of titanium and niobium create nitrides and carbonitrides, which then serve as irreversible hydrogen traps. In this way during the enamelling the hydrogen will be trapped and unable to penetrate the boundary surface and cause the fish-scales.

Titanium and niobium carbonitrides in IF-steels are the particles of incoherent character, which dispose of their own crystal lattice. The observation of substructure on carbon replicas using transmission electron microscopy confirmed the presence of small precipitates with rather incoherent interfaces. Fine precipitation particle on the basis of titanium and niobium are shown in Fig. 5. It is obvious that this kind of a trap is inadequate from the viewpoint of hydrogen absorption. Also, the larger inclusions based on the Ti-S (mostly $Ti_4C_2S_2$) are shown in Fig. 5. Due to the small size of incoherent particles, their “help” in the capture of hydrogen atoms is not expected.

4. Conclusions

- Diffusion coefficients obtained for investigated IF-steel are lower by three orders of magnitude than that in crystal lattice of α -Fe, meaning that in the examined material lots of microstructural traps were present that slowed down the transport of H-atoms.

- Permeation curves of IF-steel showed a steep slope, which indicated the fact that irreversible traps (MnS-inclusions, carbides) existed in a very small

number. This confirms the fact that the differences between diffusion parameters obtained from first permeation and other permeations are insignificantly small.

– Impedance measurements revealed that the resulting passive layer due to its small thickness could not represent a barrier to hydrogen diffusion through the membrane of IF-steel.

– The microstructure of IF-steel consists of large grains of ferrite with some cementite, known as an irreversible trap.

– By metallographic and SEM/EDS analysis of inclusions, titanium nitride was registered as the result of increased concentration of titanium in the chemical composition of IF-steel. Titanium and niobium were added in IF-steel forming precipitates that serve as irreversible hydrogen traps in order to prevent the appearance of fish scales in enamelling process.

Acknowledgements

This work was supported by the Ministry of Science, Education and Sport of the Republic of Croatia within the project 124-1241565-1524.

References

- [1] Rana, R., Bleck, W., Singh, S. B., Mohanty, O. N.: *Materials Letters*, 61, 2007, p. 2919. [doi:10.1016/j.matlet.2006.10.037](https://doi.org/10.1016/j.matlet.2006.10.037)
- [2] Bruncková, H., Kováč, F.: *Kovove Mater.*, 40, 2002, p. 53.
- [3] Mihalikova, M.: *Metallurgija*, 49, 2010, p. 161.
- [4] Valentini, R., Solina, A., Paganini, L., Degregorio, P.: *Journal of Materials Science*, 27, 1992, p. 6583. [doi:10.1007/BF01165940](https://doi.org/10.1007/BF01165940)
- [5] Nižnik, Š., Zavacký, M., Janák, G., Furman, L.: *Acta Metallurgica Slovaca*, 13, 2007, p. 336.
- [6] Liu, P. W., Wu, J. K.: *Materials Letters*, 57, 2003, p. 1224. [doi:10.1016/S0167-577X\(02\)00962-X](https://doi.org/10.1016/S0167-577X(02)00962-X)
- [7] Begić Hadžipašić, A., Malina, J., Malina, M.: *Strojarstvo*, 51, 2009, p. 529.
- [8] Zrník, J., Mamuzić, I., Dobatkin, S. V.: *Metallurgija*, 45, 2006, p. 323.
- [9] Brass, A. M., Chene, J.: *Corrosion Science*, 48, 2006, p. 3222. [doi:10.1016/j.corsci.2005.11.004](https://doi.org/10.1016/j.corsci.2005.11.004)
- [10] Devanathan, M. A. V., Stachurski, Z.: *J. Electrochem. Soc.*, 111, 1964, p. 619. [doi:10.1149/1.2426195](https://doi.org/10.1149/1.2426195)
- [11] Begić Hadžipašić, A., Malina, J., Malina, M.: *Chem. Biochem. Eng. Q.*, 25, 2011, p. 159.
- [12] Begić Hadžipašić, A., Malina, J., Nižnik, Š.: *Acta Metallurgica Slovaca*, 17, 2011, p. 129.
- [13] EN ISO 17081:2008, Method of measurement of hydrogen permeation and determination of hydrogen uptake and transport in metals by an electrochemical technique.
- [14] EN ISO 16773-1:2007, Paints and varnishes – Electrochemical impedance spectroscopy (EIS) on high-impedance coated specimens – Part 1: Terms and definitions.
- [15] EN ISO 16773-2:2007, Paints and varnishes – Electrochemical impedance spectroscopy (EIS) on high-impedance coated specimens – Part 2: Collection of data.
- [16] Park, G. A., Koh, S. U., Jung, H. G., Kim, K. Y.: *Corrosion Science*, 50, 2008, p. 341. [doi:10.1016/j.corsci.2008.03.007](https://doi.org/10.1016/j.corsci.2008.03.007)
- [17] Albert, S. K., Ramasubbu, V., Parvathavarthini, N., Gill, T. P. S.: *Sadhana*, 28, 2003, p. 383. [doi:10.1007/BF02706439](https://doi.org/10.1007/BF02706439)
- [18] Bard, A. J., Faulkner, L. R.: *Electrochemical Methods*. New York, J. Wiley & Sons 1980.
- [19] Orazem, M. E., Tribollet, B.: *Electrochemical Impedance Spectroscopy*. New Jersey, J. Wiley & Sons 2008. [doi:10.1002/9780470381588](https://doi.org/10.1002/9780470381588)
- [20] Kožuh, S., Gojić, M., Kraljić Roković, M.: *Chem. Biochem. Eng. Q.*, 22, 2008, p. 421.
- [21] Peter, L., Szucs, E., Filak, L., Vero, B., Schneider, H.: *Journal of Applied Electrochemistry*, 33, 2003, p. 613. [doi:10.1023/A:1024990905361](https://doi.org/10.1023/A:1024990905361)